Ceramics-Silikáty 67 (3), 328-333 (2023)
www.ceramics-silikaty.cz doi: 10.13168/cs.2023.0033

EFFECT OF TITANIUM SLAG PARTICLE SIZE ON THE ABILITY TO SYNTHESIZE TiO_2 BY THE HYDROTHERMAL ALKALINE DISSOLUTION METHOD

HOANG TRUNG NGON*, ***, PHAN DINH TUAN****, #KIEU DO TRUNG KIEN**, ***

*Department of Process and Equipment, Faculty of Chemical Engineering, Ho Chi Minh City University of Technology (HCMUT), 268 Ly Thuong Kiet street, District 10, Ho Chi Minh City, Vietnam
**Department of Silicate Materials, Faculty of Materials Technology, Ho Chi Minh City University of Technology (HCMUT), 268 Ly Thuong Kiet street, District 10, Ho Chi Minh City, Vietnam
***Vietnam National University Ho Chi Minh City, Linh Trung Ward, Thu Duc City, Ho Chi Minh City, Vietnam
****Research Institute for Sustainable Development, Hochiminh City University of Natural Resources and Environment, 236B Le Van Sy Street, Ward 1, Tan Binh District, Ho Chi Minh, Vietnam

#E-mail: kieudotrungkien@hcmut.edu.vn

Submitted July 5, 2023; accepted August 24, 2023

Keywords: TiO_2, Anatase, Titanium slag, Hydrothermal

Titanium slag is a by-product of iron extraction from Ilmenite ore. Titanium slag has a high TiO_2 content, so it is a suitable material for preparing TiO_2. This study investigated the influence of the slag particle size on the ability to synthesize TiO_2 by the hydrothermal alkalisation method. Three groups of titanium slag powder with average particle sizes from 18 µm to 108 µm were alkalised with a 10M NaOH solution to separate TiO_2 by the hydrothermal method. The mixing ratio by mass between the slag and the 10M NaOH solution is 1:1.5. The hydrothermal reaction was carried out at 180 °C for 7 hours. The products were analysed for their mineral, chemical, and microstructural properties using X-ray diffraction, X-ray fluorescence, scanning electron microscopy with energy-dispersive detector. The results show that the particle size significantly influences the efficiency of the TiO_2 chemical extraction from the titanium slag. The formed TiO_2 is of high purity, and the main mineral composition is anatase. The anatase polymorph of TiO_2 has the potential application as a photocatalyst and an antibacterial material.

INTRODUCTION

Titanium (Ti) is a mineral discovered in 1791 by William Gregor while analysing black magnetic sand from Menachan in Cornwall (England) [1]. Titanium is one of the rare metals with many precious properties. Titanium makes up about 0.63 wt. % of the earth's crust. The common oxide form of titanium is titanium dioxide (TiO_2). About 95 wt. % of the titanium used is in the form of titanium dioxide (TiO_2) [2]. TiO_2 has three polymorph forms: anatase, brookite, and rutile. These allotropes differ by the arrangement of the $[TiO_6]^{8-}$ octahedra [3].

TiO_2 is a commonly used chemical in many industries. Anti-corrosion materials for paints [4], fillers in the paper industry [5], and increased colour fastness for printing inks [6], etc. can be mentioned as some TiO_2 applications. TiO_2 is also a popular raw material for the ceramic industry [7]. Besides the typical applications mentioned above, TiO_2 is also widely used in high-tech fields such as electronic components [8], piezoelectric ceramic materials [9], components in the optical fibres [10], and increased brightness for LED screens [11], etc. In addition, TiO_2 with the anatase polymorph is a very popular material for photocatalytic and bactericidal applications [12].

TiO_2 is usually produced from the primary raw material of ilmenite ($FeTiO_3$) or from rutile (TiO_2) ores by different chemical methods. Among them, chlorination is the most common method that is applied. DuPont developed the first chlorination method more than 70 years ago in 1950. A. Adipuri et al. also chlorinated a mixture of iron and titanium at 1450 °C for 180 minutes to obtain pure TiO_2 [13]. Sulfuric acid is a chemical compound used to prepare TiO_2 from ilmenite and rutile ores. K. Zhu et al. found that the Ti(IV) and Fe(III) separation efficiency by this method is 99.88 wt. % and 99.90 wt. %. The purity of Ti(IV) and Fe(III) solutions are 98.75 wt. % and 99.18 wt. %, respectively [14]. In addition, high-temperature fluorination [15] and solution fluorination are also used to prepare TiO_2 [16].

The above acidification methods are often highly toxic and cause equipment corrosion. To solve the above problem, the application of the alkaline dissolution method to prepare TiO_2 is being studied and used [17]. In the alkaline dissolution method, the TiO_2 in the raw materials is dissolved in a strong alkaline solution in normal conditions [18] or in an environment with high temperature and pressure [19].

With the alkaline dissolution method, the technological parameters greatly determine the ability to synthesise TiO_2. In this study, we investigate the influence of titanium slag particle size on the ability to synthesise TiO_2 by the alkaline dissolution method. It is carried out at high temperatures and pressure. The efficiency of the reaction stages to synthesise TiO_2 was tested by techniques such as X-ray diffraction, Fourier transform infrared spectroscopy, X-ray fluorescence spectroscopy, scanning electron microscopy, and energy-dispersive X-ray spectroscopy.

EXPERIMENTAL

Materials

The used titanium slag with its chemical composition is presented in Table 1. Three different particle size groups were used to investigate the influence of the slag particle size on the ability to participate in the alkaline dissolution reaction. The average particle sizes of these three groups are 23.35 µm, 63.07 µm, and 81.06 µm, respectively, with the symbols T1, T2, and T3. The particle size distribution charts of the three groups are depicted in Figure 1.

Table 1. Chemical composition of the titanium slag (wt. %).

TiO_2	Al_2O_3	SiO_2	CaO	V_2O_5	Fe_2O_3	ZrO_2	Na_2O	Others
91.21	1.06	2.34	0.21	0.15	0.92	1.11	2.55	0.45

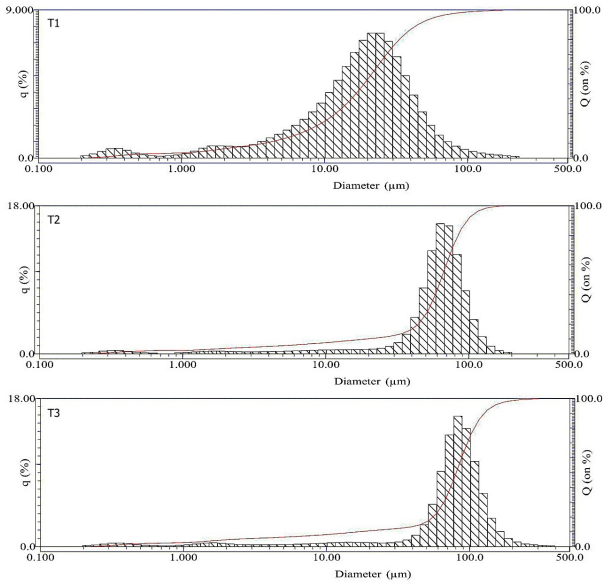

Figure 1. Particle size distribution chart of the three titanium slag groups.

Analysis method

The laser method was used to analyse the particle size distribution of the raw materials. A Horiba LA-920 laser analyser was used with the analytical conditions set according to ASTM D4464.

X-ray diffraction (XRD) was used for the mineral identification of the products. A Brucker D2 PHARSER XRD analyser was used. Analysis conditions were set as a scan range from 10 – 75°, with a scan step of 0.02, in mode C.

X-ray fluorescence (XRF) was used to determine the chemical composition of the samples. An ARL ADVANT'X XRF analyser from Thermo Fischer was used.

Scanning electron microscopy method (SEM) combined with energy dispersive X-ray spectroscopy (EDX) was used to analyse the microstructure and distribution of elemental composition on the sample surface. A Jeol JSM-IT 200 analyser was used.

Procedure

The synthesis of TiO_2 from titanium slag is carried out through three stages including:

Stage 1 – Separating TiO_2 from the titanium slag: RED slag powder is mixed with NaOH in a mass ratio 1:1.05. Water was added to ensure that the NaOH concentration reached 10 M. The mixture was stirred at 90 °C for 1 hour. Next, the mixture was submitted to the hydrothermal treatment in an autoclave at 180 °C for 7 hours. The product, after autoclaving, was filtered to separate the liquid and solid phases. The solid phase part was washed with distilled water. After drying, the chemical composition was determined by XRF and XRD methods to evaluate the ability to separate TiO_2. The solution was kept to perform the TiO_2 recovery reaction.

Stage 2 – Precipitating $TiO(OH)_2$: The solution, after the hydrothermal autoclave, was reacted with a 50 % sulfuric acid solution. An acidic solution is added until a solution reaching a pH of 6 - 7 is obtained. The process was carried out with a magnetic stirrer at 90 °C with a stirring speed of 1200 rpm. Then, distilled water is added to the mixture in a ratio of water/solution equal to 3/1 and was stirred for 2 hours. The precipitation reaction from the solution was used to obtain $TiO(OH)_2$. The precipitate was washed and filtered using a centrifuge. The minerals formed were determined by the XRD method.

Stage 3 – Calcination of $TiO(OH)_2$ at 400 °C for 2 hours obtain to form TiO_2 powder. The chemical and mineral composition of the TiO_2 powder after being calcined was determined by XRD, XRF, SEM, and EDX methods.

RESULTS AND DISCUSSION

Stage 1 – Separating TiO_2 from the titanium slag

The titanium slag samples after the hydrothermal autoclaving at 180 °C for 7 hours were analysed by XRD and XRF to evaluate the properties of the residue remaining after the reaction. The results of the XRD analysis are presented in Figure 2, in which RM (raw materials) is the symbol of the starting material. The results of the XRD analysis in Figure 2 show that there are similar minerals in the samples. With the RM sample, the XRD chart shows the presence of the minerals ilmenite ($FeTiO_3$) and titanium dioxide (TiO_2). For the samples after the hydrothermal autoclave, the XRD pattern indicates the presence of the minerals ilmenite ($FeTiO_3$), titanium dioxide (TiO_2), and hematite (Fe_2O_3). The peaks of ilmenite appeared at diffraction positions of 24.35, 32.57, 40.33, and 48.75° [20]. The peaks of the mineral titanium dioxide are present at diffraction positions of 24.35, 36.91, 48.01, and 55.03° [21]. Moreover, the mineral hematite appeared at the diffraction positions of 33.19, 57.66, and 64.08° [22].

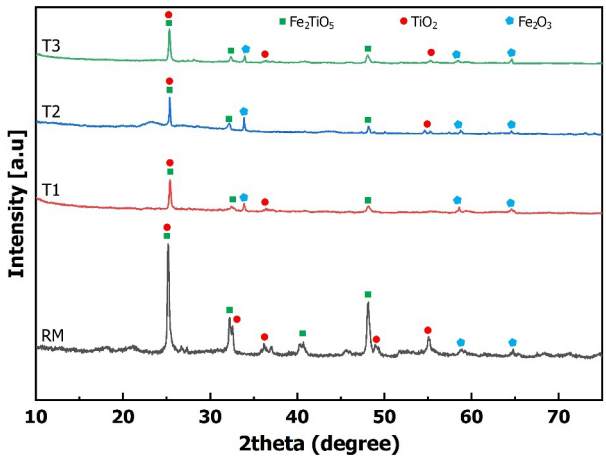

Figure 2. The XRD patterns of the titanium slag residue

However, there was an apparent change in the intensity of the samples before and after the hydrothermal reaction. In the T1, T2, and T3 samples, the intensity of the peaks related to TiO_2 and $FeTiO_2$ were reduced compared with that of the RM sample - especially the peaks associated with the TiO_2 minerals. The intensity decrease is evident at diffraction positions of 22.45, 32.57, 36.91, 48.01, and 55.03°. In contrast to the intensity reduction of the above peaks, some peaks related to hematite are clearly observed (33.19, 57.66, and 64.08°). This result proves that TiO_2 in the titanium slag participated during the hydrothermal process and caused the peaks of this mineral to decrease on the XRD patterns. The chemical reaction Equations (1, 2) describe the reaction process of TiO_2 with the NaOH solution in a hydrothermal environment. Thanks to the decrease in the intensity of the TiO_2 peaks and the formation of Fe_2O_3 from the reaction (1), the peaks of Fe_2O_3 increase in the T1, T2, and T3 spectra.

$$FeTiO_3 + NaOH + H_2O \rightarrow Fe_2O_3 + Na_2O{\cdot}nTiO_2{\cdot}mH_2O \quad (1)$$

$$TiO_2 + NaOH + H_2O \rightarrow Na_2O{\cdot}nTiO_2{\cdot}mH_2O \quad (2)$$

Where n and m are coefficients

The results of the XRD patterns show the ability of the hydrothermal environment to dissolve TiO_2 in the titanium slag by NaOH. However, the XRD patterns did not show a clear difference in the reactivity of the T1, T2, and T3 samples. To further clarify this difference, the post-reaction samples were analysed by XRF to determine the remaining TiO_2 content in the slag. The lower the TiO_2 content in the slag, the greater the ability to dissolve TiO_2 to form $Na_2O{\cdot}nTiO_2{\cdot}mH_2O$. The results of determining the TiO_2 content in the slag after the reaction are shown in Figure 3. Figure 3 shows that all the samples have reduced TiO_2 contents after participating in the hydrothermal reaction. The results again demonstrate the reactivity of TiO_2 in the slag with the NaOH solution. The results also show that the TiO_2 solubility reactivity increases as the slag particle size decreases. As the particle size decreases, the contact surface between the solid phase (titanium slag) and the liquid phase (NaOH solution) increases. Thanks to this, the ability to dissolve TiO_2 is also increased. This conclusion also shows that reducing the slag particle size is one of the methods that can be applied to improve the efficiency of the TiO_2 recovery reaction from the titanium slag.

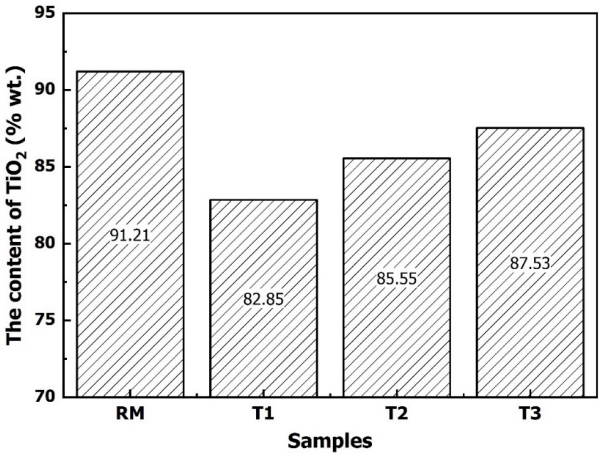

Figure 3. The TiO_2 composition of the titanium slag residue.

Stage 2 - Precipitating $TiO(OH)_2$

The precipitate in the second stage was washed and dried. The dried samples were subjected to an XRD analysis. Figure 4 shows the results of the XRD patterns of the samples. The XRD patterns indicate that

the primary mineral formed after precipitation from the solution is titanium oxyhydroxide ($TiO(OH)_2$). The characteristic diffraction peaks for $TiO(OH)_2$ are at 26.77, 32.28, 37.22, 48.35, and 55.32° [23]. Many studies have shown that $TiO(OH)_2$ is the precursor of the TiO2 generation by different solution methods [24-26]. The appearance of $TiO(OH)_2$ in the solution after precipitation also demonstrated the ability to extract TiO_2 from the titanium slag by the alkaline dissolution method. The similar XRD patterns of the samples also show that the particle size of the titanium slag does not significantly affect the precipitation of $TiO(OH)_2$ from the alkaline solution.

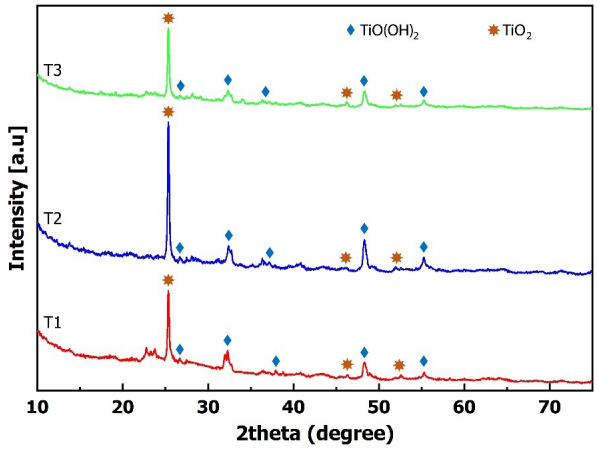

Figure 4. The XRD patterns of the $TiO(OH)_2$ powders.

Besides $TiO(OH)_2$, the XRD patterns show the TiO_2 minerals at diffraction positions 25.22, 47.85, and 53.72°. Except for the peak at position 25.42°, the appearance of the remaining peaks is not clear. The appearance of these peaks indicates the formation of TiO_2 microcrystals during the precipitation process. TiO_2 microcrystals react with water and are rapidly converted to $TiO(OH)_2$ according to reaction (3). Therefore, pyrolysis is necessary for synthesising TiO_2 by the solution method.

$$TiO_2* + H_2O \rightarrow TiO(OH)_2 \quad (3)$$

Stage 3 – Calcination to form a TiO_2 powder

After precipitation, the $TiO(OH)_2$ powder was calcinated at 400 °C to separate the water and form TiO_2. Figure 5 shows the XRD analysis result of the TiO_2 powder after calcination.

Similar to the XRD patterns in Figure 4, the XRD patterns in Figure 5 also show the formation of $TiO(OH)_2$ and TiO_2. However, the appearance of peaks corresponding to these two minerals has changed. The peaks corresponding to $TiO(OH)_2$ are only present at

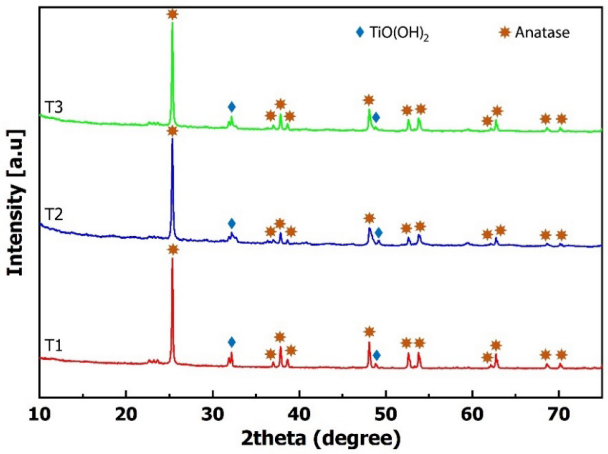

Figure 5. The XRD patterns of the TiO_2 powders.

32.28 and 48.35° positions. This result proves that TiO_2 was formed from the dehydrating reaction of $TiO(OH)_2$ at 400 °C according to reaction (4). The appearance of TiO_2 at the diffraction peaks at positions 25.22, 36.86, 37.72, 38.46, 47.85, 53.72, 54.89, 61.92, 62.51, 68.59, and 70.05° shows that the TiO_2 formed is anatase polymorph.

$$TiO(OH)_2 \rightarrow TiO_2 + H_2O \quad (4)$$

The morphology of the anatase was also examined by a scanning electron microscope (SEM). Figure 6 shows the SEM image result of the formed anatase powders. The SEM image results show that the TiO_2 powders have similar shapes. The formed body is spherical which have a particle size ranging from 10 to 20 nm. The results also show that the alkaline dissolution method in a hydrothermal environment can produce anatase on a nanoscale. The nano-sized spherical particles help to increase the specific surface of the anatase. Many studies

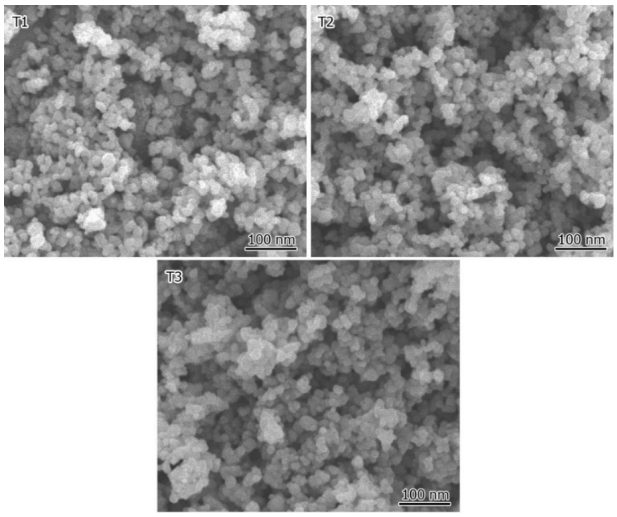

Figure 6. The morphology image of the TiO_2 powders.

have also shown that nano-anatase has a reduced band gap [27]. From there, the anatase nanoparticles can be easily stimulated through a photocatalytic effect using only the visible light band [28].

Besides the morphological observation, the elemental distribution and chemical composition of the TiO_2 powder was also analysed by EDX and XRF methods. Figure 7 shows the result of the elemental composition distribution map, and Figure 8 shows the composition of the samples.

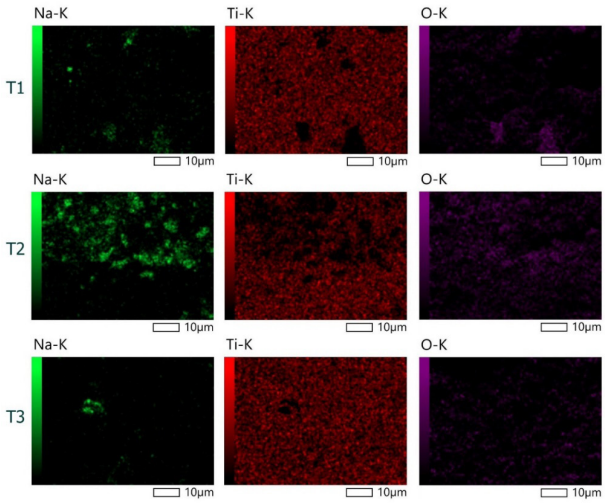

Figure 7. The elemental distribution map of the TiO_2 powders.

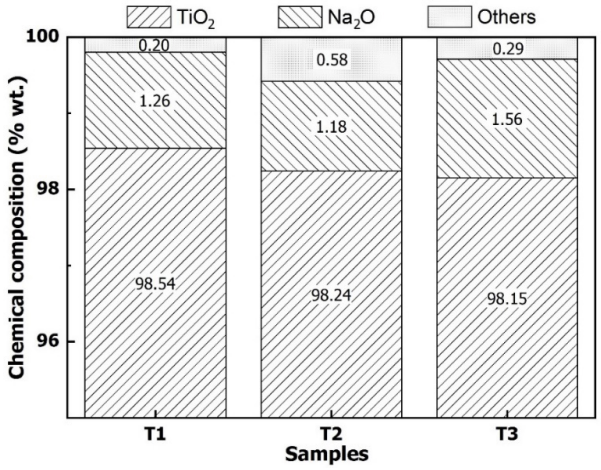

Figure 8. The chemical composition of the TiO_2 powders.

The analysis results of the element distribution map shown in Figure 7 and the chemical composition shown in Figure 8 give similar results. All the samples have the main chemical composition of TiO_2 with a relatively high purity (with TiO_2 accounting for 98.15 - 98.54 wt. %). The difference in the TiO_2 content of the samples from T1 to T3 is also insignificant, indicating that the particle size of the raw materials does not significantly influence the chemical composition of the formed TiO_2 powder. In addition, TiO_2 synthesised by the alkaline dissolution method will also be mixed with impurities such as Na_2O. Na_2O is the remaining component due to the incomplete washing process.

CONCLUSIONS

In this study, TiO_2 was synthesised from three different groups of titanium slag by the alkaline dissolution method in a hydrothermal device. The results showed that the group of particles with an average size of 23.35 μm gave the most significant TiO_2 recovery (8.36 wt. %). Although the material's particle size dramatically affects the ability to separate TiO_2 from the titanium slag, it does not significantly affect the crystallisation ability to form $TiO(OH)_2$ from the alkaline solution. It also does not significantly affect the purity and the allotropic form of the TiO_2 formed after dehydrating at 400 °C. The purity of TiO_2 obtained is above 98 wt. %, and the main allotropic form of TiO_2 is anatase. The resulting TiO_2 has a particle size ranging from 10 to 20 nm. Anatase nanoparticles can help the TiO_2 photocatalyst reaction under visible light.

Acknowledgment

We acknowledge the Ho Chi Minh City University of Technology (HCMUT), VNU-HCM for supporting this study.

REFERENCES

1. Gázquez M. J., Bolívar J. P., García-Tenorio García-Balmaseda R., Vaca F. (2014): A review of the production cycle of titanium dioxide pigment. *Materials Sciences and Applications, 5*, 441-458. Doi: 10.4236/msa.2014.57048
2. Li M., Geng Y., Liu G., Gao Z., Rui X., Xiao S. (2022): Uncovering spatiotemporal evolution of titanium in China: A dynamic material flow analysis. *Resources, Conservation and Recycling, 180*, 106166. Doi: 10.1016/j.resconrec.2022.106166
3. Yin H., Wada Y., Kitamura T., Kambe S., Murasama S., Mori H., Sakata T., Yanagida S. (2001): Hydrothermal synthesis of nanosized anatase and rutile TiO_2 using amorphous phase TiO_2. *Journal of Materials Chemistry, 11*, 1694-1703. Doi:10.1039/B008974P
4. Sathiyanarayanan S., Azim S. S., Venkatachari G. (2007): Corrosion protection of magnesium ZM 21 alloy with polyaniline–TiO_2 composite containing coatings. *Progress in Organic Coatings, 59*, 291-296. Doi:10.1016/j.porgcoat.2007.04.004
5. Park J.-K., Kim J.-K., Kim H.-K. (2007): TiO_2–SiO_2 composite filler for thin paper. *Journal of Materials Processing Technology, 186*, 367-369. Doi:10.1016/j.jmatprotec.2006.12.004
6. Braun J. H., Baidins A., Marganski R. E. (1992): TiO_2 pigment technology: a review. *Progress in organic coatings,*

20, 105-138. Doi:10.1016/0033-0655(92)80001-D
7. Teixeira S., Bernardin A. M. (2009): Development of TiO_2 white glazes for ceramic tiles. *Dyes and Pigments, 80*, 292-296. Doi:10.1016/j.dyepig.2008.07.017
8. Ashery A.(2022): The Negative Capacitance of a Novel Structure Au/PPy-MWCNTs/TiO_2/Al_2O_3/p-Si/Al. *ECS Journal of Solid State Science and Technology, 11*, p. 073008. Doi:10.1149/2162-8777/ac8076
9. Yang W., Yu. Y., Starr M. B., Yin X., Z., Kvit A., Wang S., Zhao P., Wang X. (2015): Ferroelectric polarization-enhanced photoelectrochemical water splitting in TiO_2–$BaTiO_3$ core–shell nanowire photoanodes. *Nano letters, 15*, 7574-7580. Doi:10.1021/acs.nanolett.5b03988
10. Chauhan M., Singh V. K. (2023): TiO_2 coated tapered optical fiber SPR sensor for alcohol sensing application. *Journal of Optics, 1-11*. Doi:10.1007/s12596-023-01131-y
11. Tong Y., Wang Q., Liu X., Mei E., Liang X., Xiang W. (2022): The promotion of TiO_2 induction for finely tunable self-crystallized $CsPbX_3$ (X = Cl, Br and I) nanocrystal glasses for LED backlighting display. *Chemical Engineering Journal, 429*, p. 132391. Doi:10.1016/j.cej.2021.132391
12. Li Z., Wang S., Wu J., Zhou W. (2022): Recent progress in defective TiO_2 photocatalysts for energy and environmental applications. *Renewable and Sustainable Energy Reviews, 156*, p. 111980. Doi:10.1016/j.rser.2021.111980
13. Adipuri A., Li Y., Zhang G., Ostrovski O. (2011): Chlorination of reduced ilmenite concentrates and synthetic rutile. *International Journal of Mineral Processing, 100*, 166-171. Doi:10.1016/j.minpro.2011.07.005
14. Zhu K., Ren X., Li H., Wei Q. (2021): Simultaneous extraction of Ti (IV) and Fe (III) in HCl solution containing multiple metals and the mechanism research. *Separation and Purification Technology, 257*, p. 117897. Doi:10.1016/j.seppur.2020.117897
15. Stovpchenko G., Lisova L., Medovar L., Goncharov I. (2023): Thermodynamic and Physical Properties of CaF_2–(Al_2O_3–TiO_2–MgO) System Slags for Electroslag Remelting of Inconel 18 Alloy. *Materials Science, 58*, 494-504. Doi:10.1007/s11003-023-00690-6
16. Gordienko P., Dostovalov V., Pashnina E. (2017): Hydrofluoride method of complex processing of titanium-containing raw materials. *Solid State Phenomena, 265*, 542-547. Doi:10.4028/www.scientific.net/SSP.265.542
17. Chen J., Guo S., Omran M., Gao L., Zheng H., Chen G. (2022): Microwave-assisted preparation of nanocluster rutile TiO_2 from titanium slag by NaOH-KOH mixture activation. *Advanced Powder Technology, 33*, p. 103549. Doi:10.1016/j.apt.2022.103549
18. Han Y. F., Sun T. C., Li J., Wang L. N., Xue T. Y., Qi T. (2012): Removing of Si in the NaOH molten salt reaction of titanium slag to produce TiO_2. *Advanced Materials Research, 418*, 387-392. Doi:10.4028/www.scientific.net/AMR.418-420.387
19. Wang D., Chu J., Liu Y., Li J., Xue T., Wang W., Qi T. (2013): Novel process for titanium dioxide production from titanium slag: NaOH-KOH binary molten salt roasting and water leaching. *Industrial & Engineering Chemistry Research, 52*, 15756-15762. Doi:10.1021/ie400701g
20. Lv W., Lv X., Xiang J., Wang J., Lv X., Bai C., Song B. (2017): Effect of pre-oxidation on the carbothermic reduction of ilmenite concentrate powder. *International Journal of Mineral Processing, 169*, 176-184. Doi:10.1016/j.minpro.2017.09.008
21. Xing Y., Li X., Guo X., Li W., Chen J., Liu Q., Xu Q., Wang Q., Yang H., Shu Y., Bi X. (2020): Effects of Different TiO2 Nanoparticles Concentrations on the Physical and Antibacterial Activities of Chitosan-Based Coating Film, *Nanomaterials, 10*, p.1365. Doi:10.3390/nano10071365
22. Niederberger M., Krumeich F., Hegetschweiler K., Nesper R. (2002): An iron polyolate complex as a precursor for the controlled synthesis of monodispersed iron oxide colloids. *Chemistry of Materials, 14*, 78-82. Doi:10.1021/cm0110472
23. Zhang C., Zhou Y., Zhang Y., Zhang Z., Xu Y., Wang Q. (2015): A 3D hierarchical magnetic Fe@Pt/$Ti(OH)_4$ nanoarchitecture for sinter-resistant catalyst. *RSC Advances, 5*, 64951-64960. Doi:10.1039/C5RA13887F
24. Byranvand M. M., Kharat A. N., Fatholahi L., Beiranvand Z. M. (2013): A review on synthesis of nano-TiO_2 via different methods. *Journal of nanostructures, 3*, 1-9. Doi:10.7508/JNS.2013.01.001
25. Gupta S. M., Tripathi M. (2021): A review on the synthesis of TiO_2 nanoparticles by solution route. *Central European Journal of Chemistry, 10*, 279-294. Doi:10.2478/s11532-011-0155-y
26. Zhu Y., Zhang L., Gao C., Cao L. (2000): The synthesis of nanosized TiO2 powder using a sol-gel method with $TiCl_4$ as a precursor. *Journal of Materials Science, 35*, 4049-4054. Doi:10.1023/A:1004882120249
27. Avinash B. S., Chatumukha V. S., Jayanna H. S., Naveen C. S., Rajeeva M. P., Harish B. M., Suresh S., Lamani A. R. (2016): Effect of particle size on band gap and DC electrical conductivity of TiO_2 nanomaterial. *AIP conference proceedings, 1728*, p. 020426. Doi:10.1063/1.4946477
28. Kien K. D. T., Minh D. Q., Minh H. N., Nhi N. V. U. (2023): Synthesis of TiO_2-SiO_2 from tetra-n-butyl orthotitanate and thetraethyl orthosilicate by the sol-gel method applied as a coating on the surface of ceramics. *Ceramics–Silikáty, 67,* 58-63. Doi:10.13168/cs.2023.0002